Adsorption and binding dynamics of graphene-supported phospholipid membranes using the QCM-D technique

D. A. Melendrez, T. Jowitt, M. Iliut, A.F. Verre, S. Goodwin and A. Vijayaraghavan

Supplementary Information

Experimental

Overview

The successful formation of uniform supported lipid membranes demands following a standardized procedure. Here, we describe the experimental steps to prepare Small Unilamellar Vesicles (SUVs), to condition the QCM-D system, present them to selected substrates and acquire the frequency and dissipation responses for further analysis.

Reagents

For Graphene Oxide (GO) preparation: Hydrogen Peroxide (H_2O_2) 30% (Sigma Aldrich), Sulphuric acid (H_2SO_4) 98% (Sigma Aldrich), Sodium Nitrate ($NaNO_3$) 98% (Alfa Aesar), Potassium Permanganate (KMnO4) 98% (Alfa Aesar)

For buffer preparation: Milli-Q water (>18 MΩ), 1,2-dioleoyl-sn- glycero-3-phosphocholine (DOPC) lipid (Avanti Polar Lipids), Biotinyl Cap dispersed in Chloroform (10 mg/mL, Avanti Polar Lipids), Avidin protein from egg white (Sigma Aldrich), Analytical grade HEPES buffer (Acros Organics), NaCl (powder, Sigma Aldrich), $MgCl_2$ (powder, Sigma Aldrich), NaOH (pellets, Fischer Scientific), H_2O_2 (30% solution), Ammonia (25% solution, Sigma Aldrich),

For cleaning: Sodium dodecyl sulphate (Fischer Scientific), Hellmanex II (Hellma Analytics).

Graphene oxide preparation

Graphene oxide used in this work was prepared according to a modified Hummers method described in ref. (1). Briefly, graphite flakes of 50 mesh (1g) and $NaNO_3$ (0.9 g) were mixed in concentrated H_2SO_4 (34 ml) in a round bottom flask and kept overnight to intercalate. Then the mixture was cooled down in an ice bath and 4.5 g $KMnO_4$ where added slowly under constant stirring. The resulting mixture was left for 5 days at RT for graphite oxidation. After oxidation process was complete, the resulting brown slurry was diluted at a slow rate with 100 ml H_2SO_4 solution of 5% after which 10 ml of H_2O_2 solution of 30% was added dropwise. Finally, the dispersion was further diluted with 100 ml mixture of H_2SO_4/H_2O_2 of 3%/0.5%. The resulted graphite oxide was purified via centrifugation process by repeated washing with diluted H_2SO_4 and then DI water until the pH of the supernatant was close to neutral. The homogenisation and complete exfoliation of graphene oxide was performed using a vertical stirrer at a low speed for ~1h. The stock solution of GO (8.1 mg/mL) was diluted to a concentration value of 0.5 mg/mL.

Buffer solution

The buffer solution is prepared diluting 10 mM HEPES, 100 mM NaCl, and 5mM $MgCl_2$ in MilliQ water. The pH is adjusted to 7.4 with a 1M NaOH solution when necessary. Stir this solution for at least 2 hours to ensure complete dissolution. To increase the pH, add dropwise the sodium hydroxide solution during gentle stirring until a stable value is reached. Filter the buffer with the 0.2 µm nylon membranes. Store the buffer in the fridge for up to two weeks.

Cleaning solutions

For cleaning the QCM-D system and quartz crystals, prepare both 2% SDS and Hellmanex II solution in MilliQ water. A strong cleaning solution for gold crystals (QSX-301) is prepared as a 5:1:1 mixture of MilliQ water, Ammonia (25%) and Hydrogen Peroxide.

Lipid vesicle preparation (and Biotin caps incorporation)

To obtain DOPC SUVs follow the next procedure.

Thoroughly rinse the inner walls of a 5-mL glass vial with chloroform using chloroform syringes. Dry the vial using a soft beam of N_2. Take 1 mL from DOPC lipid dispersed in chloroform (2.5 mg/mL) and pour it in the clean vial. *Note*: for Biotin caps incorporation, take 25 µL of this vitamin dispersed in chloroform and mix it in the same vial. Dry the chloroform with a soft beam of N_2 until complete evaporation. Hydrate the lipid (/vitamin) with 1 mL of HEPES buffer solution. Fill a 1 mL extruder syringe with the hydrated lipid (/vitamin). Place one 50 nm polycarbonate filtering membrane (Nalgene) at the middle of the Teflon receptacle of the extruder, add two spacers per side and tightly close the hex nut. Insert another clean and empty 1 mL syringe on the opposite side of the Teflon receptacle. Extrude the dispersed lipid for at least 23 times. Be gentle to avoid tearing the filtering membrane. It is recommended to use freshly made lipid vesicles to avoid vesicle aggregation.

Initial preparation of Quartz Crystals

These cleaning procedures are based on the protocol provided by QSense (2). The sensors used in this study are QCM with gold surface (QSX-301) and with Silicon Dioxide (QSX-303)/Silicon Dioxide 300nm (QSX-318). A teflon QCM cleaning holder (Q-Sense, QCLH 301) was used to prevent scratches on the surface.

SiO_2 QCM chips

The following cleaning steps are regarded as mild cleaning and also applies for the gold crystals as a routine cleaning procedure.

1. UV/ozone treat for 10 minutes.
2. Immerse the sensor surfaces in the solution of 2% SDS and sonicate them for 15 minutes.
3. Rinse the sensors with abundant MilliQ water.
4. Immerse the sensors in MilliQ water and sonicate them for 15 minutes.
5. Immerse the sensors in 99% ethanol and soak them for 10 minutes.
6. Dry the surfaces using a mild beam of nitrogen gas.
7. UV/ozone treat for 25 minutes.

Au QCM chips

- Chemical treatment (Ammonium Peroxide Mix)

This cleaning process should be carried out under a fumes hood, wearing adequate PPE.

1. Using wash bottles, squirt the following solutions over the working electrode: 10% Decon 90, acetone and isopropanol. Use DI water between each solution to rinse well the surface.
2. Treat the crystals under UV/ozone atmosphere for 10 minutes.
3. Heat the strong cleaning solution for gold to 75 º C.
4. Place the sensor in the heated solution for 5 minutes.
5. Rinse the sensors with MilliQ water. Keep the surfaces wet after ammonium-peroxide immersion until they are rinsed well with water.
6. Dry with nitrogen gas.
7. UV/ozone treat for 25 minutes.

- Surfactant treatment

Follow the same cleaning steps for silicon dioxide sensors.

Coating QCM-D crystals with GO

In order to coat the Au/SiO_2 crystals, the following methodology must be applied after completing the appropriate cleaning procedure.

1. Configure the following parameters in the spin coating machine (SCM) (Laurell technologies Corp. WS-650MZ-23NPPB)

   Speed = 3500 rpm, acceleration = 350 rpm/sec, time = 120 sec.
2. Place a QCM crystal in the vacuum nuzzle of the SCM.
3. Drop cast 70 µl of GO (0.5 mg/ml) on the surface of the Au/SiO_2 QCM working electrode. Let the solution settle for 30 seconds.
4. Close the lid of the SCM and start the spinning.
5. Repeat steps 2-4 once for each set of crystals.

Thermal reduction of GO-coated crystals

This procedure requires to preheat the oven before cleaning and coating the desired number of sensors since the heating curve from each oven may vary. In our case, the oven was set at 180ºC to preheat 1 hour before placing the chips to be reduced.

Follow the next procedure immediately after the spin coating of crystals is completed.

1. Distribute the selected chips to be reduced in petri dishes and label them accordingly.
2. When the over reaches 180 ºC place the petri dishes with the chips inside the chamber and close the door tightening the screw to ensure good vacuum.
3. Leave the samples for 20 hours.
4. After 20 hours shut down the heater, turn off the vacuum pump and slowly turn the intake valve from the vacuum oven to the *open* position. *Note*: to avoid blowing away the chips inside the oven, turn the valve gently until the atmospheric pressure fills the chamber.
5. Let the chamber cool down for a few minutes and wearing heat gloves carefully take the QCM chips with Teflon tweezers holding them from the edges.
6. Store the crystals in order inside holding boxes for a safe transport.

QCM-D measurement procedure

Initial system cleaning and priming

The following steps are intended to be applied on the Q-Sense Omega Auto (Biolin Scientific) system, which consists of 8 sensing ports automatically fed through customized scripts.

- Thorough ports and tubing cleaning

a. Load all ports with clean maintenance sensors. *Note*: verify the right position of the sensor matching the anchor symbol.

b. All the ports (1-8) must be initially washed by running 2% SDS at a flow rate[1] of 25 μL/min for at least 10 min. This step should remove all remaining lipids and biological material from all tubing and syringes.

c. Rinse with system liquid[2] for at least 15 min.

d. Flow 2% Hellmanex through the system for at least 10 min.

e. Finally rinse with system liquid for at least 15 min.

f. Remove the maintenance sensors, rinse the chamber with MilliQ water.

- Sensors & ports priming

Eliminating trapped bubbles is crucial to obtain a stable baseline and a steady response via continuous buffer flow.

a. Load the chamber with the desired number of sensors to be used. Up to four chips can be used for a parallel data acquisition. Ensure that the electrodes are all dry during placement to avoid any variations during measurements.

b. Set the chamber temperature to 24 ºC to minimize thermal drift.

c. Run system liquid through the loaded ports until a stable baseline is noticeable. *Note*: despite this step can be programmed to automatically stop when a stable baseline is reached it is recommended to run it manually to override the baseline criteria from the system.

d. Vacuum ports and start running buffer solution through the working sensors for at least 5 min before the actual sample injection and *vesicle fusion* technique is applied.

[1] All flow rates are equal to 25 μL/min unless specified.

[2] *System liquid* refers to ultrapure water.

Formation of supported lipid membranes using the vesicle fusion technique

The aim of these steps is to present lipid vesicles to QCM-D sensors with different working-electrode surfaces by flowing Small Unilamellar Vesicles (SUVs) dispersed in buffer solution. An initial vesicle-substrate interaction is expected to be followed by a vesicle-vesicle interaction to obtain specific structures of lipid membranes. This procedure has been successfully applied to obtain bilayers on clean hydrophilic substrates such as SiO_2 and monolayer on modified Au (3). The adsorption and formation of all the lipid membranes discussed in this work was accomplished by following the same experimental steps.

1. Deposit the extruded lipid vesicles dispersed in buffer in a 1.5 mL vial and place it in the right-hand rack and lock the lid from the Omega Auto system. *Note*: in case of carrying out a binding event, also place in the rack a vial containing 100 µL of protein dispersed in chloroform, then dried and finally hydrated with 900 µL of HEPES buffer.
2. Run buffer solution through the desired chips for at least 5 min. Start recording the frequency and dissipation responses from this step. *Note*: verify the stability and flatness of the baseline during this time. In case that some harmonics show jumps and high variation this may indicate the presence of bubbles in the system and/or a bad interface between the working electrode and the media. To solve this, redo steps *c* and *d* from the priming section.
3. After 5 min of stability inject the lipid vesicles (0.1 mg/mL) to the desired chips during 10 minutes. *Note*: The system will indicate the quantity of lipid in buffer solution required to complete this step, however 1.0 mL should be enough to run 4 parallel measurements with the same parameters described here. In case that the vial is not filled to the right level, the system will automatically stop the execution of the script.
4. Verify the resonant frequency and dissipation values in liquid. Right after lipid injection a frequency shift must occur showing some mass uptake and an increase in the energy dissipation. Depending on the type of membrane being formed the frequency shift will stabilize to a specific value. *Note*: using a control chip is highly recommended to verify the validity of the experimental procedure. A well-known adsorption kinetics is that for a bilayer on bare SiO_2 where the values from Fig. 2a (main text) are expected, with a tolerance of $\Delta f \pm 1$ Hz and $\Delta D \pm 0.5 \times 10^{-6}$.
5. Rinse the lipid layer with buffer for at least 5 min to remove any excess lipid and homogenize the membrane.
6. If performing the binding measurement, inject the Avidin from the vial (after SLM stabilization) and let it settle under continuous flow for at least 5 min.
7. Rinse all sensors with buffer to eliminate any excess protein and/or material deposited on the surface and to record complete values for further analysis.
8. When the main body of the analytical script is completed, the system will run a wash routine. During these steps, all the material present on the sensors will be removed and the surfaces, syringes and tubing will be washed using the selected surfactants (Hellmanex and/or SDS) and finally rinsed with system liquid.
9. Upon completion, the door can be opened and the sensors can be taken out of the chamber.
10. It is recommended to leave the chamber clean and dry to be ready to use in subsequent experiments.

Samples characterization

The atomic force microscopy (AFM) of the GO and rGO was performed using a Bruker Dimension FastScan probe microscope operating in taping mode. The tips used for the surface scanning were aluminium coated silicon FastScan-A tips from Bruker. For coated crystals characterization, the diluted GO dispersion (0.5 mg/mL) was casted on clean QCM-D substrates and spin coated as previously described.

The scanning electron microscopy (SEM) was performed on a SEM Zeiss Ultra setup, using an accelerating voltage of 5 kV.

The X-ray photoelectron spectroscopy (XPS) data were collected on a SPECS custom built system composed of a Phobios 150 hemispherical electron analyser with 1D detector. The X-ray source is a microfocus monochromated Al K-alpha (1486.6eV) source. All spectra were collected with a pass energy of 20eV. Combined ultimate resolution as measured from Ag 3d is 0.5eV with X-ray source and 20eV pass. The XPS data processing was done using CasaXPS software (version 2.3.16 PR 1.6). The C1s region peak fitting was done using Gaussian/Lorentzian shape components (for sp^3 carbon) and asymmetric shape components (for sp^2 carbon) respectively. XPS C1s region was fitted with the synthetic components in the manner which minimizes the total square error fit and corresponds to the literature reports. In the case of rGO, it was impossible to distinguish between sp^2 and sp^3 carbons, therefore the signal was fitted with a single asymmetric component. The GO sample for XPS was prepared by drop casting the dispersion on a clean Si/SiO2 (300nm) and drying in a vacuum oven to achieve a film thickness not less than 10 nm. The rGO sample was prepared using the same conditions used for the reduction of GO on QCM crystals. The GO vas first casted and dried on the Si/SiO2 (290 nm) substrate, followed by the reduction in vacuum at 180 ºC for 20 hours.

Raman spectrum was taken on a Renishaw Raman system equipped with a Leica microscope and a CCD detector. Raman spectrum was recorded using 532 nm laser line (Cobolt SambaTM continuous wave diode-pumped solid-state laser, 20 mW), and the laser power was kept below 10 µW to avoid thermal degradation of the samples. 30 spectra per sample was taken. The relative intensity ratio ($\boldsymbol{I_D/I_G}$) was measured from the averaged acquired mappings.

Results and discussion

Contact angle

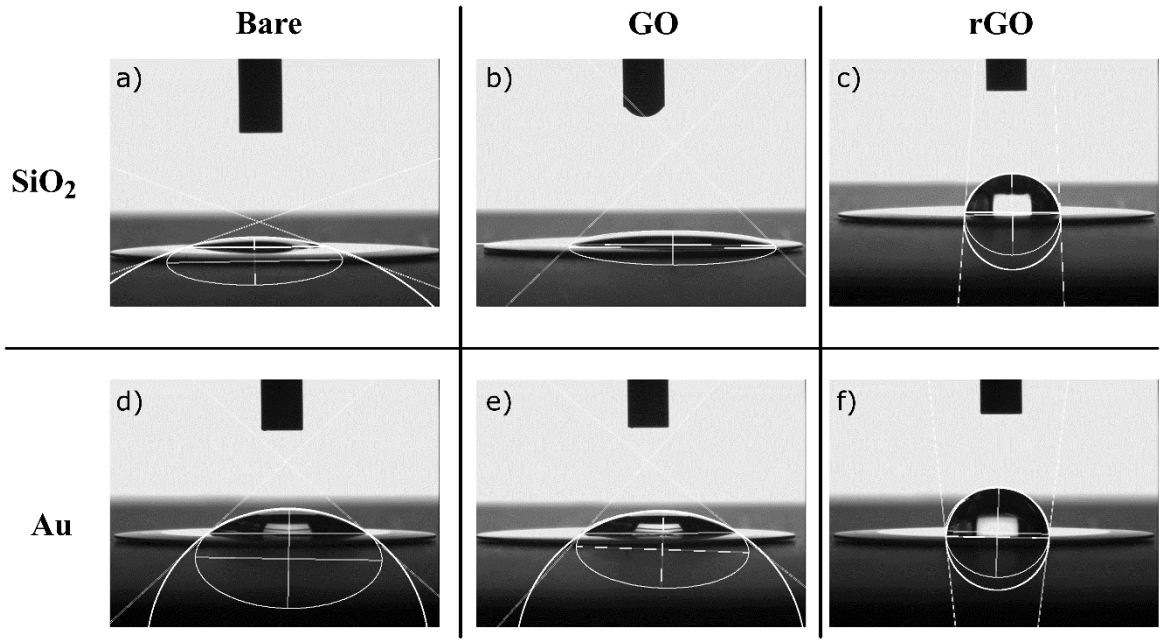

Fig.S1 Contact angle sheet. **a-f**) Manual fit of the water droplet using the ImageJ plugin [ref]

The wetting contact angles for the range of QCM crystals is shown in Fig. S1. The manual circle-ellipse fittings were computed using an ImageJ software plugin developed and published by Marco Brugnara (4) for such specific task. The software works on pre-captured high contrast images of sessile drops which are processed by first inverting the image upside down, namely, the water droplet must be pending from the top of the image, then two points are selected for the baseline of the droplet and finally three edge points that follow the curvature of the droplet are selected. On each case, 5 readings were captured for statistical effects and the results given by the script are shown in Tables S1 and S2. Table S1 shows the results for the SiO_2 crystal variations (Fig. a-c) while Table S2 shows the results obtained for the Au crystal variations (Fig. d-f). In both cases the highlighted cells show the final average value for the ellipse fitting from which the standard deviation showed a lower value than that obtained for the circle fitting.

Crystal type	Theta C	Uncertainty	Theta Left	Theta Right	Theta E	Circle StDev	Ellipse StDev
SiO_2 - bare	15.8	0.1	20.7	18.8	19.8	8.56E-02	8.92E-04
	14	0.1	16.6	13.5	15	1.16E-01	2.98E-03
	14	0.2	18.6	14	16.3	2.03E-01	2.27E-03
	13.3	0.1	14.9	13.4	14.2	1.06E-01	2.73E-03
	15.1	0.2	21.8	21	21.4	2.35E-01	2.15E-03
Averages	**14.44**	**0.14**	**18.52**	**16.14**	**17.34**	**1.49E-01**	**2.20E-03**

Crystal type	Theta C	Uncertainty	Theta Left	Theta Right	Theta E	Circle StDev	Ellipse StDev
SiO_2 - GO	25.3	0.3	38.3	34.4	36.4	4.31E-01	4.19E-04
	24.8	0.3	35.4	34.7	35	5.50E-01	6.91E-04
	24.2	0.2	30.8	33	31.9	3.40E-01	9.99E-04
	24.9	0.1	30	27.7	28.8	2.38E-01	7.16E-04
	25	0.2	25.3	31.7	28.5	3.72E-01	6.09E-04
Averages	**24.84**	**0.22**	**31.96**	**32.3**	**32.12**	**3.86E-01**	**6.87E-04**

Crystal type	Theta C	Uncertainty	Theta Left	Theta Right	Theta E	Circle StDev	Ellipse StDev
SiO_2-rGO	82.6	0.6	89.2	92.6	90.9	8.19E-01	1.16E-04
	82.8	0.4	88.5	89.2	88.8	5.10E-01	5.43E-04
	78.8	0.4	86.3	89.2	87.8	4.90E-01	3.60E-04
	79.5	0.3	87.2	86.2	86.7	3.64E-01	5.18E-04
	80.8	0.5	87.9	88	88	6.14E-01	5.47E-04
Averages	**80.9**	**0.44**	**87.82**	**89.04**	**88.44**	**5.59E-01**	**4.17E-04**

Table S1 Manual fitting results for SiO_2 crystal set using the Contact Angle ImageJ plugin. Shadowed cell value is the final angle.

Crystal type	Theta C	Uncertainty	Theta Left	Theta Right	Theta E	Circle StDev	Ellipse StDev
Au - bare	34	0.2	42.2	42.2	42.2	3.10E-01	3.86E-04
	34.4	0.3	41.6	39.7	40.7	3.82E-01	4.88E-04
	34.3	0.3	38.7	41.2	40	3.99E-01	8.96E-04
	34.2	0.3	40.9	42.5	41.7	4.51E-01	7.15E-04
	34	0.3	40.3	43.6	42	4.62E-01	4.44E-04
Averages	**34.18**	**0.28**	**40.74**	**41.84**	**41.32**	**4.01E-01**	**5.86E-04**

Crystal type	Theta C	Uncertainty	Theta Left	Theta Right	Theta E	Circle StDev	Ellipse StDev
Au - GO	32.2	0.3	38.8	40	39.4	3.88E-01	5.83E-04
	32.7	0.2	40.9	39.4	40.2	3.59E-01	7.46E-04
	32.3	0.2	36.8	38.4	37.6	2.61E-01	8.18E-04
	32.2	0.2	35	38.1	36.6	3.26E-01	8.88E-04
	32	0.3	35.6	37.9	36.8	4.86E-01	4.74E-04
Averages	**32.28**	**0.24**	**37.42**	**38.76**	**38.12**	**3.64E-01**	**7.02E-04**

File Name	Theta C	Uncertainty	Theta Left	Theta Right	Theta E	Circle StDev	Ellipse StDev
Au - rGO	87.4	0.3	94.6	93.9	94.2	4.74E-01	5.58E-04
	87.2	0.4	97.1	96.1	96.6	6.32E-01	1.18E-04
	87.2	0.4	95.7	94.4	95.1	5.23E-01	8.16E-05
	88.1	0.3	94.9	95.8	95.4	5.06E-01	2.56E-04
	86.7	0.3	92.2	92.6	92.4	4.11E-01	1.69E-04
Averages	**87.32**	**0.34**	**94.9**	**94.56**	**94.74**	**5.09E-01**	**2.37E-04**

Table S2 Manual fitting results for Au crystal set using the Contact Angle ImageJ plugin. Shadowed cell value is the final angle.

SEM images

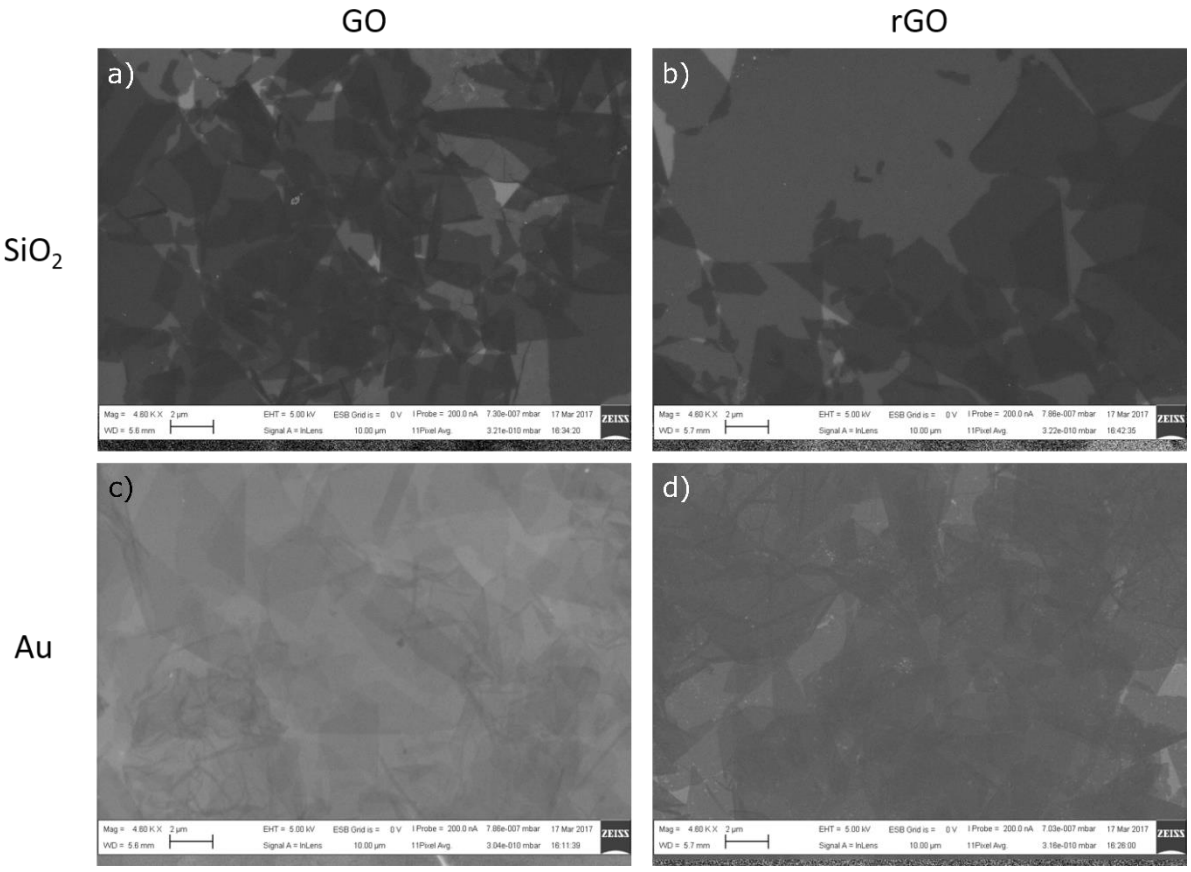

Fig.S2 Scanning Electron Microscope (SEM) showing GO and rGO flakes arrangement on: **a)** on GO-SiO_2 **b)** rGO-SiO_2, **c)** GO-Au **d)** rGO-Au. Probe voltage 5.00 kV

The SEM images of the SiO_2 and Au QCM crystals coated with GO (Fig S2 a) and c)) show full coverage of the substrate with flakes, with the number of layers (determined from the contrast and further AFM) ranging from single to few layers overlaps, which is unavoidable when using spin coating deposition technique. The reduction of the GO (Fig S2 b) and d)) doesn't seem to affect the substrate coverage and the flakes density. However, in case of Au substrate (Fig S2 d)) the rGO flakes present many small holes (which is not an SEM artifact), unlike rGO present on SiO_2. Considering the identical reduction conditions for both samples, we speculate that the gas evolution during the GO reduction, combined with high temperature (180 ºC) could have contributed to the Au etching which, in turn, contributed to the holes formation.

AFM images

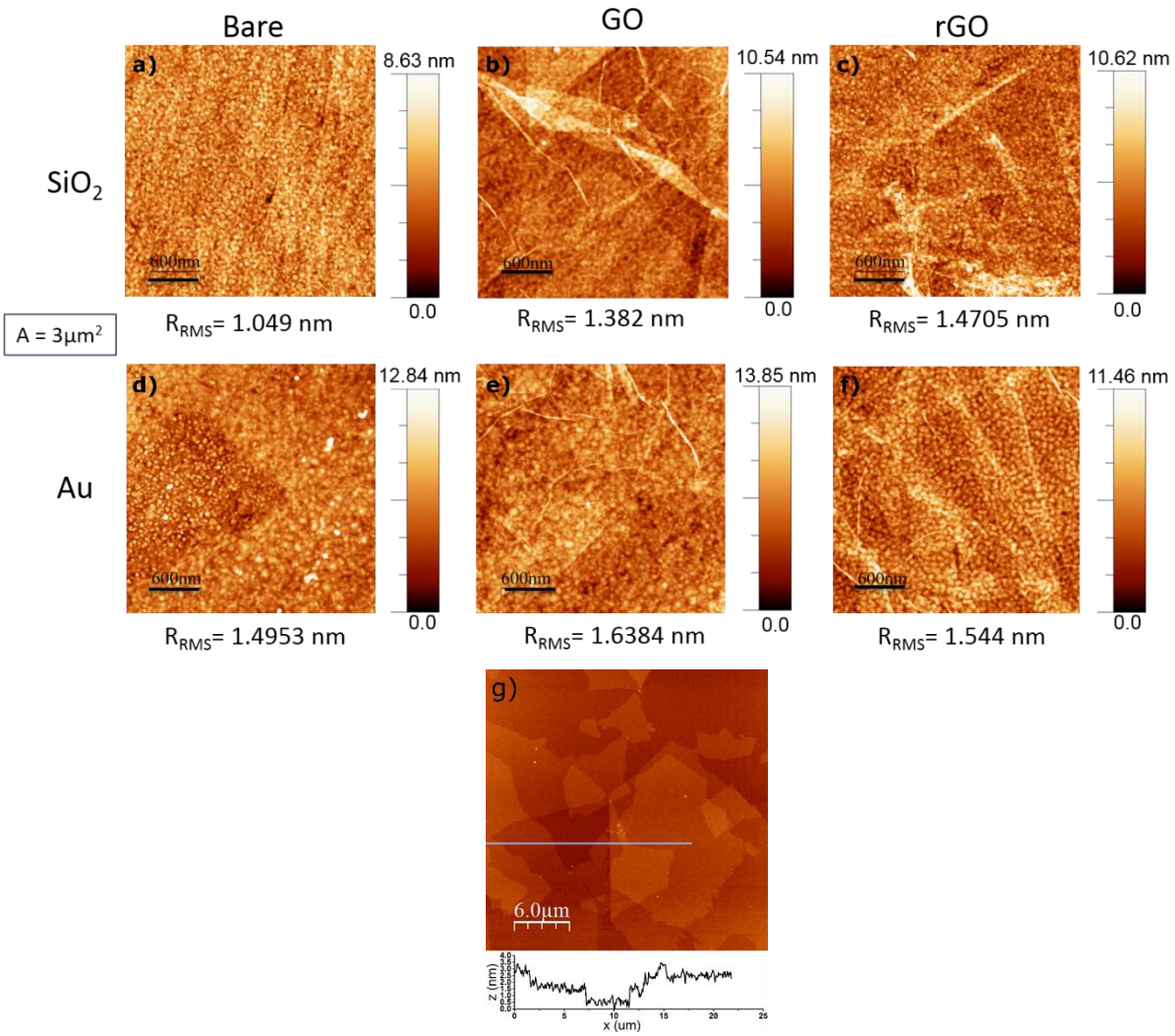

Fig. S3 AFM mappings of full crystal set. Root-mean-square roughness (R_{RMS}) and height profile values in nm scale are shown for: **a)** bare SiO_2, **b)** GO-SiO_2, **c)** rGO-SiO_2, **d)** bare Au, **e)** GO-Au and **f)** rGO-Au. Scan area in all images is 3µm^2, **g)** shows the AFM image of GO reference sample on Si/SiO2 (290 nm) wafer for a 30/30 um surface scan. The AFM height profile shows a thickness of ~1nm for single layer flakes which increases almost proportionally with the number of flakes.

The topographical characterization of the prepared crystals was performed through Atomic Force Microscopy (AFM) to obtain a height profile and values for the root-mean-square roughness (R_{RMS}) for each crystal. The influence of the latter parameter on the response of the QCM has been stressed in different studies, comprising from the variation between a modeled frequency shift and experimental values of different RMS roughness levels (5), to the effect on the lipid-substrate interaction on the formation of structurally different areas of the same lipid composition (6). It has been shown that surface roughness affects the mechanisms of vesicle rupture and, in some cases, the formation of Supported Lipid Bilayers (SLBs) on solid supports (7), however SLB formation is only slightly affected on the nanometer scale. Therefore, controlling the roughness of a surface has direct impact on the structure of the membrane formed on top of the selected substrate. In fact, a rough crystal surface may effectively damp more the response of the frequency shift than a smooth polished crystal.

The AFM images for three individual SiO_2 and three Au crystals are presented in Fig S3. Each sample was carefully prepared by following the same steps and under similar conditions, as described in experimental section. Because the AFM scan has limited surface scan range, the information about the flakes distribution on the surface and the quality of the coverage are provided mainly be the SEM images. As the SEM showed, both, SiO_2 and Au QCM crystals are fully covered with GO/rGO with very few small empty spots, and from number of GO/rGO layers ranging mainly from single to 3 layers. The monolayer character of the original GO is confirmed by the reference sample (Fig S3 g)). However, it is difficult to ascribe in AFM the exact position or the number of layers present on the SiO_2 and Au QCMs substrates because of their high surface roughness (Fig S3 a) and d)) and the tendency of GO/rGO sheets to flatten on the surface and take its shape (Fig S3 b), c), e) and f)).

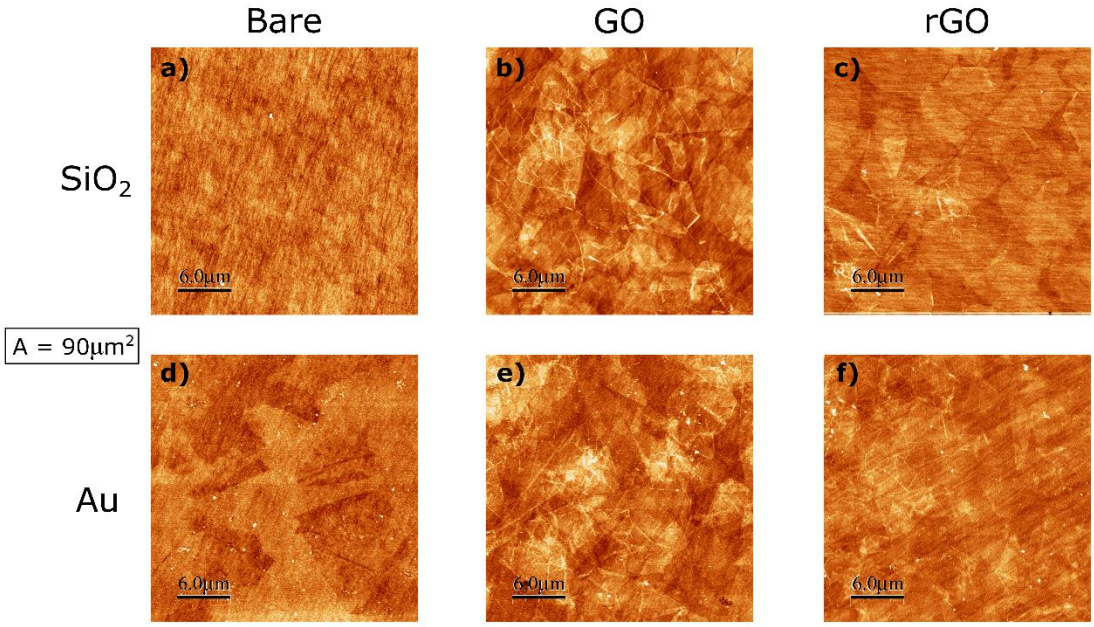

Fig. S4 Large scan AFM mappings of full crystal set. **a)** bare SiO_2, **b)** GO-SiO_2, **c)** rGO-SiO_2, **d)** bare Au, **e)** GO-Au and **f)** rGO-Au. Scan area in all images is 90 μm^2.

The only reference of the flakes presence is detected by their crumbles, overlaps and creases formed during the spin coating and drying process, as can be seen clearly in lower resolution AFM images from Fig. S3.

As it can be seen from Fig S4 a), b) and c) the R_{RMS} value of the surface increases with the addition of GO on the Si. A careful inspection of the Si-GO, however, shows that the roughness coming from the SiO_2 is slightly "smoothened" when the GO is present. This can be ascribed to the higher thickness of the flakes given by the functional groups and the water molecules trapped between the substrate and GO, between the GO flakes, and on the surface, due to the hydrophilic nature of GO. The increased R_{RMS} value is probably given by the contribution of the wrinkles, folds and overlaps of GO flakes to the existing roughness. In case of Si-rGO substrate, the roughness of the substrate seems very similar to the bare Si. An explanation would be the reduction in thickness of the GO flakes upon the reduction process accompanied by the dehydration. These, together with the wrinkled nature of the rGO flakes, will contribute to a higher R_{RMS} value compared to bare Si and GO.

The intrinsic higher roughness of the Au substrate (Fig S4 d)) doesn't change significantly with the addition of GO (Fig S4 e)). Unlike the case of SiO_2, in this case the GO coated Au seems to keep the roughness characteristics and the only contribution to the slightly increased R_{RMS} value is the roughness generated by the flakes, at, however, lower rate than in case of SiO_2. This can be due to the difference in GO – substrate interaction, as well as more hydrophobic nature of Au which leads to a better dehydration between GO and substrate. After the thermal reduction, the R_{RMS} values for the Au-rGO (Fig S4 f)) are lower than Au-GO and slightly higher than bare Au. A close look at the AFM scan (Fig. S4 f)) reveals that the deposited Au "islands" present on Au-rGO have a more flat and uniform character compared to the initial Au substrate. This can be due to a slight Au etching during the high temperature reduction of GO, which would explain lower roughness compared to Au-GO sample.

XPS on GO and rGO coated substrates

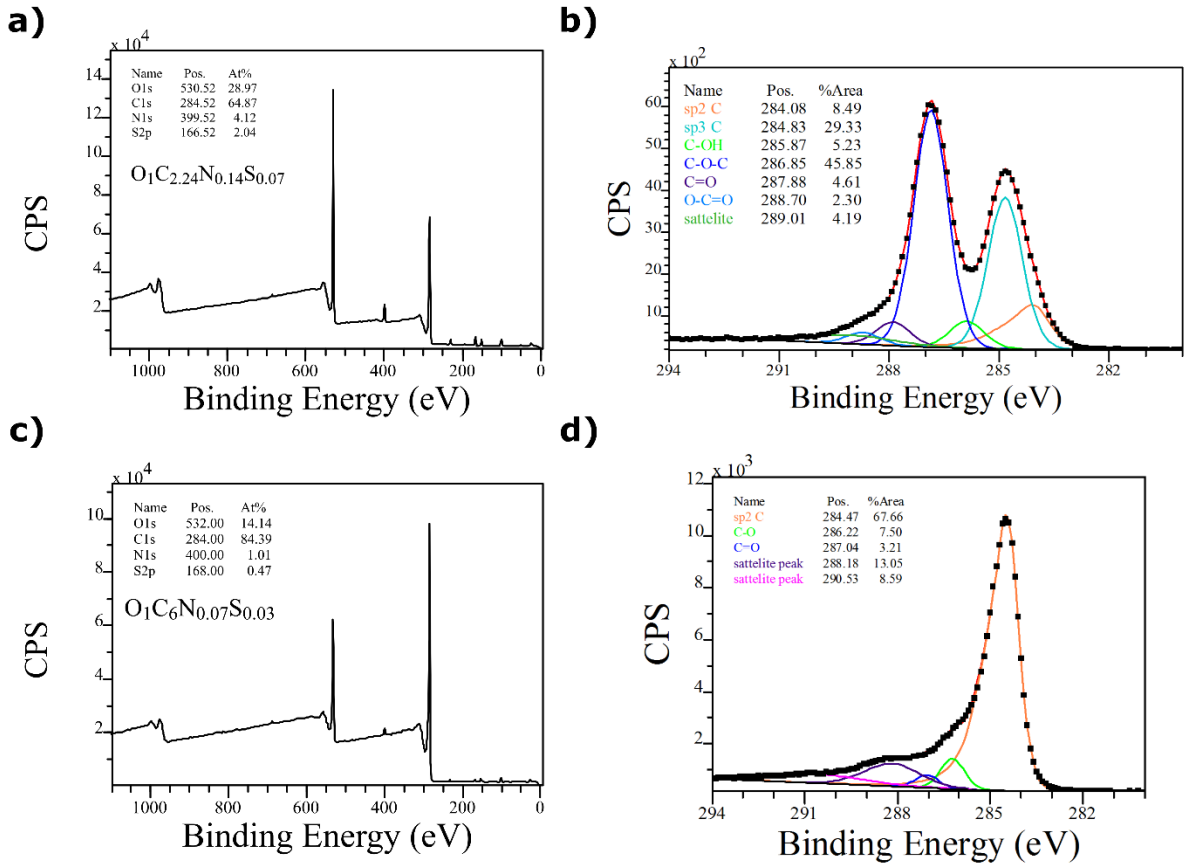

Fig. S5 XPS of coated samples **a)** wide scan GO, **b)** deconvoluted C1s of GO, **c)** wide scan rGO, **d)** deconvoluted C1s of rGO.

The XPS technique was performed to reveal the nature of chemical bonds in GO and to monitor their evolution after GO reduction. Fig S5 a), b), c) and d) represent the wide scan and C1s spectra of GO and rGO respectively. The wide scan of GO reveals a C to O ratio of ~2, in accordance with the literature for GO (8) with small amounts of nitrogen and Sulphur impurities. After reduction (Fig. S5 c)) the C to O ratio increases significantly to 6. The C1s spectrum of the GO (Fig. S5 b) shows the presence of different functional groups decorating the basal plane and the edges of GO: hydroxyl (C-OH) and epoxy (C-O-C) groups between ~285 and 287 eV, carbonyl (C=O) and carboxyl (O-C=O) groups between ~287 and 289 eV, and finally, sp^2 and sp^3 carbons – around ~284 eV. After reduction (Fig S5 d)) the rGO presents fewer oxygen groups, i.e. single and double carbon –oxygen groups with a binding energy of ~286 and 287 eV respectively, and an increased intensity sp^2 carbon peak. This proves the reduction of GO to rGO and a significant restoration of sp^2 carbons.

Raman mappings

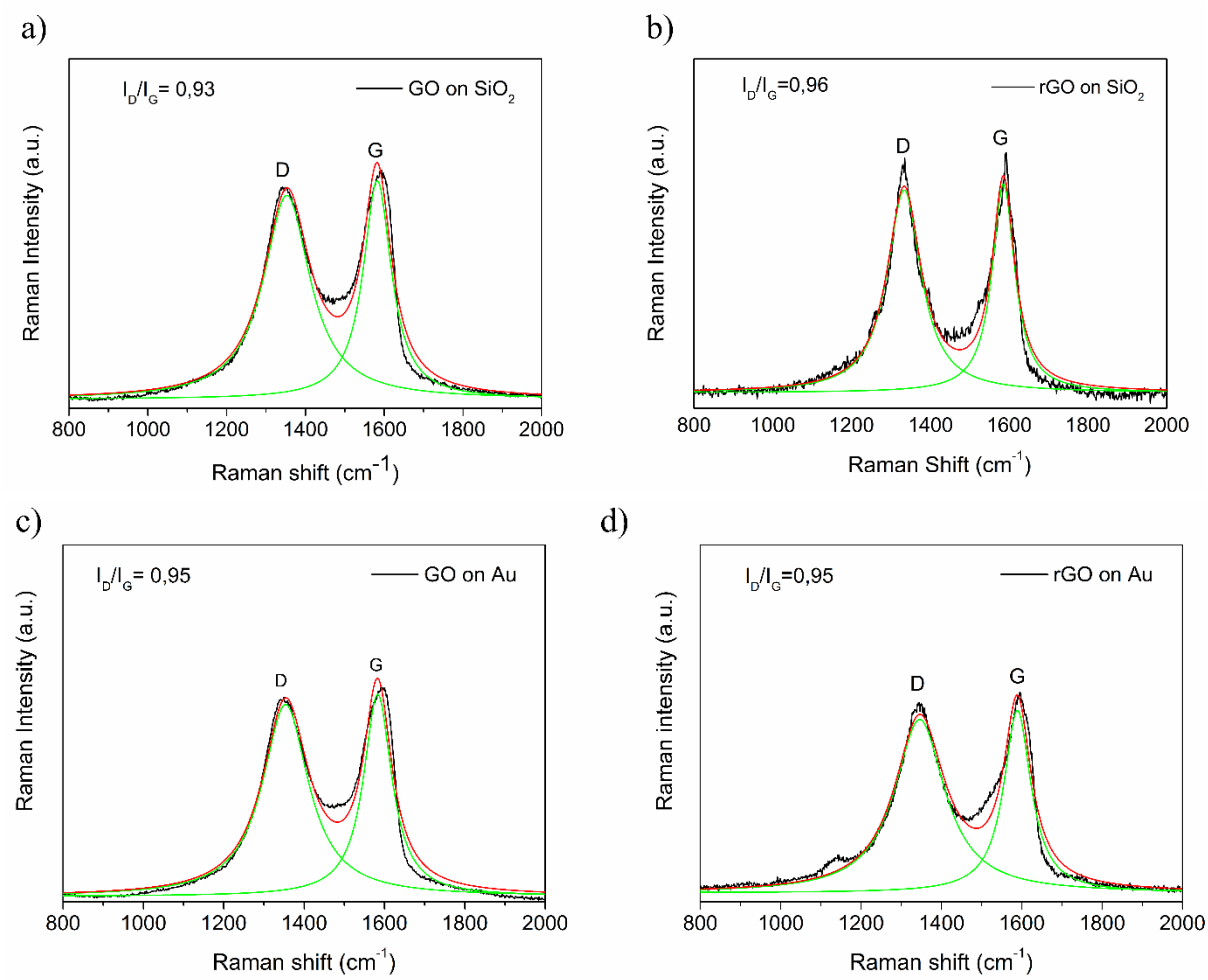

Fig S6. Raman spectra (with fits for G and D peak components) of (a) SiO_2 surface with GO coating, (b) SiO_2 surface with rGO coating, (c) Au surface with GO coating and (d) Au surface with rGO coating. Green curves show peak fits and the red curves show the sum of the peak fits (color online version).

Raman is a powerful technique used for the characterization of the graphitic materials, providing information about number of layers, lattice defects, doping etc. (9,10). Fig S6 shows the Raman spectra of GO and rGO coated QCM sensors prepared as described before. Peak fit is shown on the curves in green (online version). One of the spectral features of graphene is associated with the optical phonon mode, which occurs around ~ 1580 cm^{-1} and is called the G band (10). The D peak is associated with defects in the structure (sp^3 bonding) appears at ~ 1350 cm^{-1} (11). The relative intensity of D to G provides an indicator for determining the in-plane crystallite size or the amount of disorder in the sample, indicating the sp^2/sp^3 carbon ratio, ergo, it shows the disorder or the restoration of the graphene lattice (9,12).

Figures S6 a) and b) show the Raman spectra of GO and rGO on SiO_2-QCM-D sensors, respectively. The I_D/I_G value of 0.96 suggests the presence of graphitic domains after the reduction process in SiO_2 (Fig. S6 b)) while the ratio obtained for GO is equal to 0.93 (Fig. S6 a)). Similarly, Figures S6 c) and d) show the Raman spectra for GO and rGO, respectively, on Au-QCM-D sensors. The I_D/I_G ratio on Fig. S6 c) and d) remains equal according to our data fit, suggesting equivalent defectiveness and the absence of any damage due to the reduction process on the scanned regions. Overall, these Raman spectra indicates the presence of graphene and graphene-like domains on the selected substrates.

Overall frequency and dissipation values (3rd, 5th & 7th harmonics)

Bare substrates

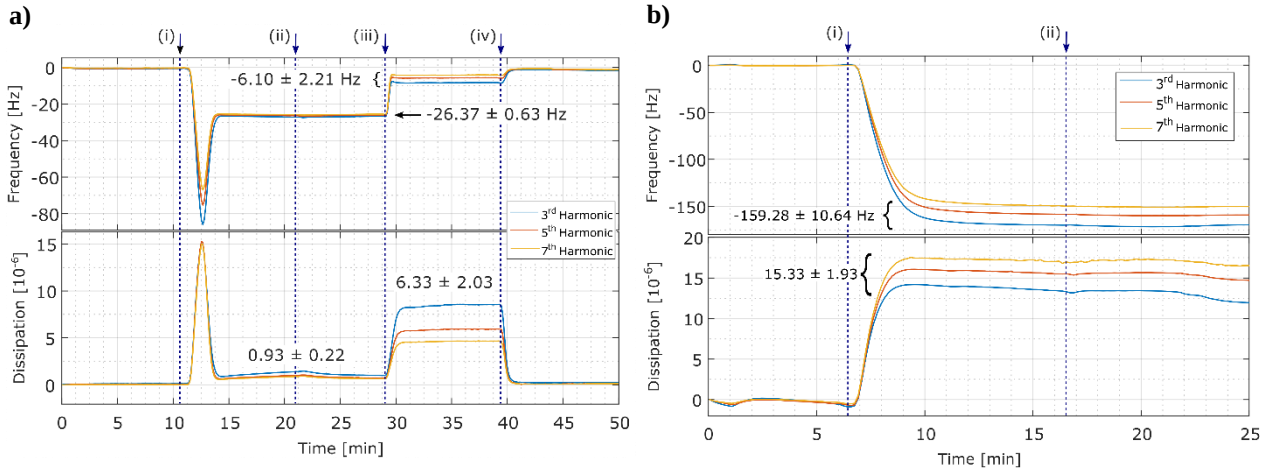

Fig.S7 Adsorption of DOPC **a)** on bare SiO_2 **b)** on bare Au. Steps: (i) injection of DOPC then (ii) buffer rinse, (iii) SDS wash, (iv) final buffer rinse.

GO coated substrates

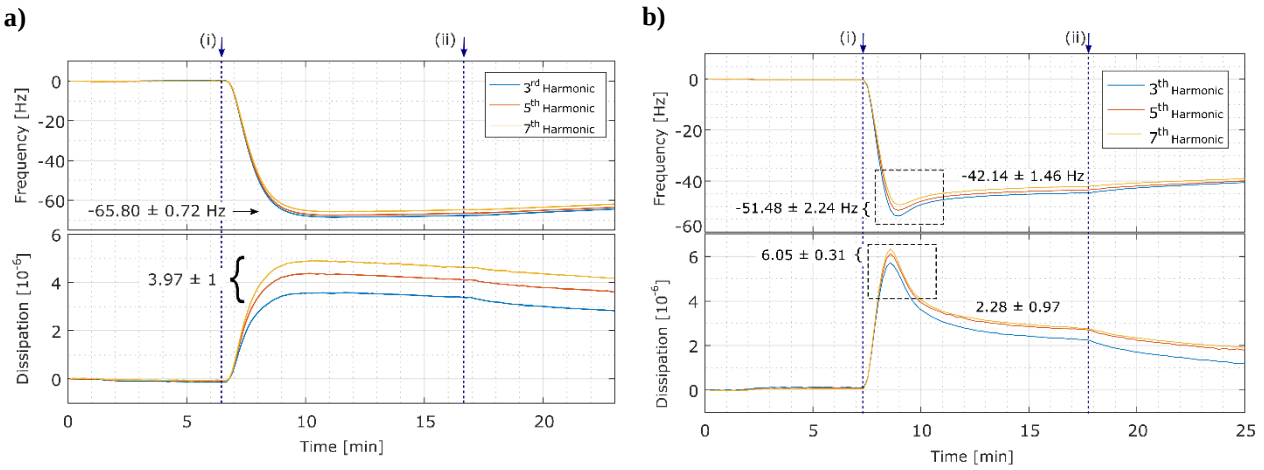

Fig.S8 Adsorption of DOPC **a)** on GO-SiO_2 **b)** on GO-Au. Steps: (i) injection of DOPC then (ii) buffer rinse

rGO coated substrates

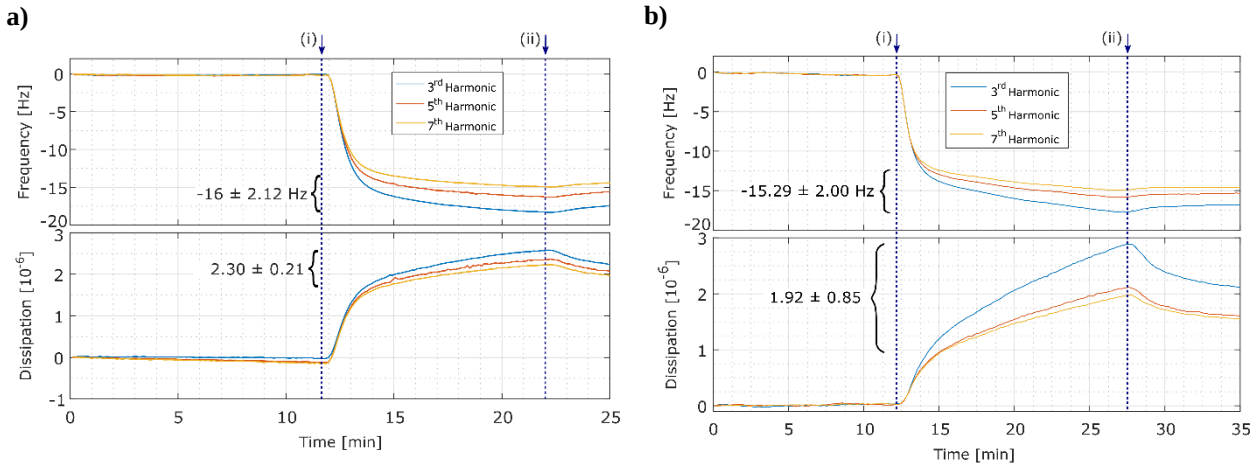

Fig.S9 Adsorption of DOPC **a)** on rGO-SiO_2 **b)** on rGO-Au. Steps: (i) injection of DOPC then (ii) buffer rinse

Binding event on bare substrates

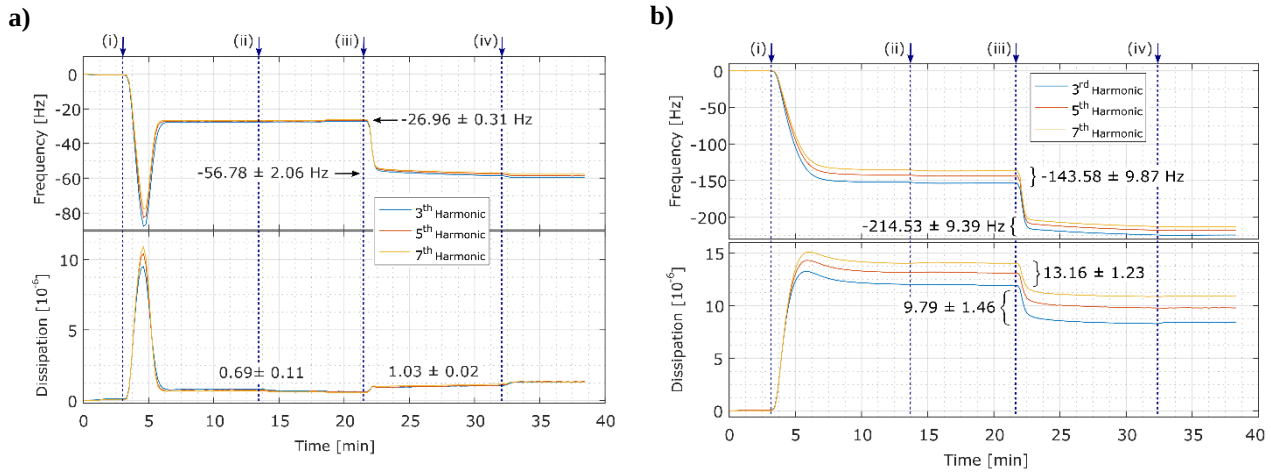

Fig.S10 Biotin-Avidin binding event on **a)** a lipid bilayer on SiO_2 **b)** intact vesicles on Au. Steps: (i) injection of DOPC then (ii) buffer rinse (iii) Avidin injection, (iv) final buffer rinse

Binding event on rGO-coated substrates

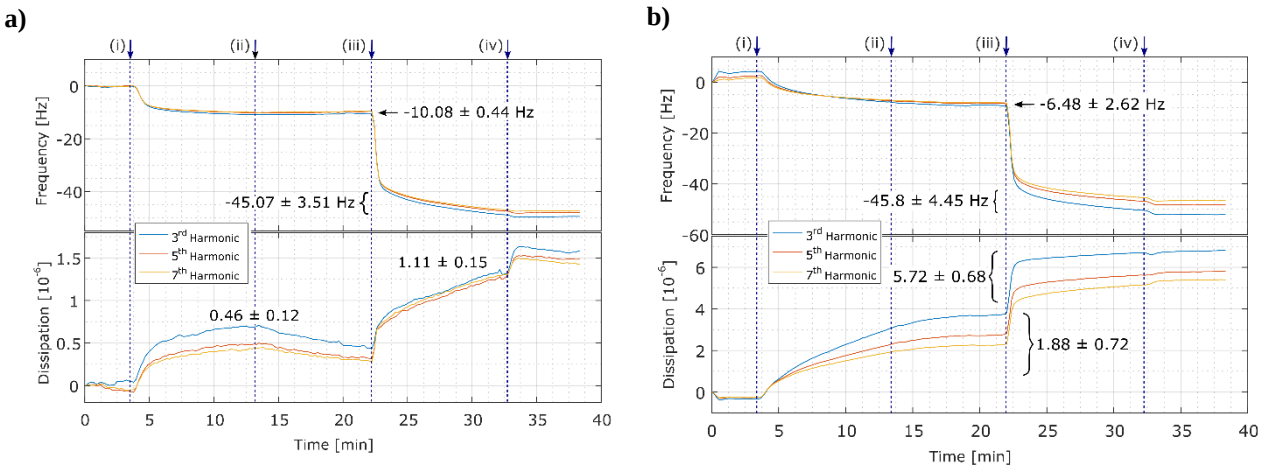

Fig.S11 Biotin-Avidin binding event on **a)** a lipid monolayer on rGO-SiO_2 **b)** a lipid monolayer on rGO-Au. Steps: (i) injection of DOPC then (ii) buffer rinse (iii) Avidin injection, (iv) final buffer rinse

References

1. Rourke JP, Pandey PA, Moore JJ, Bates M, Kinloch IA, Young RJ, et al. The real graphene oxide revealed: Stripping the oxidative debris from the graphene-like sheets. Angew Chemie - Int Ed. 2011;50(14):3173–7.

2. Scientific B. http://www.biolinscientific.com/q-sense/products/?card=QP1. 2015.

3. Keller CA, Kasemo B. Surface specific kinetics of lipid vesicle adsorption measured with a quartz crystal microbalance. Biophys J [Internet]. 1998;75(3):1397–402. Available from: http://dx.doi.org/10.1016/S0006-3495(98)74057-3

4. Marco Brugnara (marco.brugnara at ing.unitn.it). Contact Angle Plugin. 2006.

5. Rechendorff K, Hovgaard MB, Foss M, Besenbacher F. Influence of surface roughness on quartz crystal microbalance measurements in liquids. J Appl Phys. 2007;101(11).

6. Yoon T-Y, Jeong C, Lee S-W, Kim JH, Choi MC, Kim S-J, et al. Topographic control of lipid-raft reconstitution in model membranes. Nat Mater [Internet]. 2006;5(4):281–5. Available from: http://www.ncbi.nlm.nih.gov/pubmed/16565710

7. Richter RP, Bérat R, Brisson AR. Formation of solid-supported lipid bilayers: An integrated view. Langmuir. 2006;22(8):3497–505.

8. Yu H, Zhang B, Bulin C, Li R, Xing R. High-efficient Synthesis of Graphene Oxide Based on Improved Hummers Method. Sci Rep [Internet]. 2016;6(1):36143. Available from: http://www.nature.com/articles/srep36143

9. Dresselhaus MS, Jorio A, Saito R. Characterizing graphene, graphite, and carbon nanotubes by Raman spectroscopy. Annu Rev Condens Matter Phys. 2010;1(1):89–108.

10. Childres I, Jauregui L, Park W, Cao H, Chen Y. Raman Spectroscopy of Graphene and Related Materials. New Dev Phot Mater Res [Internet]. 2013;1–20. Available from: https://www.physics.purdue.edu/quantum/files/Raman_Spectroscopy_of_Graphene_NOVA_Childres.pdf

11. Sobon G, Sotor J, Jagiello J, Kozinski R, Zdrojek M, Holdynski M, et al. Graphene oxide vs. reduced graphene oxide as saturable absorbers for Er-doped passively mode-locked fiber laser. Opt Express. 2012;20(17):19463–73.

12. Iliut M, Leordean C, Canpean V, Teodorescu C-M, Astilean S. A new green{,} ascorbic acid-assisted method for versatile synthesis of Au-graphene hybrids as efficient surface-enhanced Raman scattering platforms. J Mater Chem C [Internet]. 2013;1(26):4094–104. Available from: http://dx.doi.org/10.1039/C3TC30177J